Available online at www.sciencedirect.com
ScienceDirect
Geomorphology 78 (2006) 207–221
GEOMORPHOLOGY
www.elsevier.com/locate/geomorph

Ultra-rapid landscape response and sediment yield following glacier retreat, Icy Bay, southern Alaska

Andrew Meigs [a,*], William C. Krugh [a], Kelsay Davis [a], Greg Bank [b]

[a] Department of Geosciences, Oregon State University, Corvallis, OR 97331, USA
[b] Department of Geology, Virginia Polytechnic and State University, Blacksburg, VA 24061-0420, USA

Received 18 August 2005; received in revised form 7 January 2006; accepted 10 January 2006
Available online 17 February 2006

Abstract

Glacial retreat and opening of Taan Fjord (an arm of Icy Bay, Alaska) in the last two decades drove a base level fall of ~400 m at the outlets of four tributary valleys in the region of the current Tyndall Glacier terminus. Response in the tributary valleys to this base level fall includes evacuation of stored sediment, incision of slot gorges into bedrock, and landsliding on valley walls. Fluvial transfer of eroded bedrock, glacial deposits, and stored nonglacial fluvial deposits after 1983 resulted in progradation of fan deltas toward the fjord centerline at the outlet of each of the four catchments. In the largest nonglacial tributary valley, ~0.08 km^3 (~8%) of the 0.59 km^3 of >500-m-thick stored fluvial and colluvial deposits has been transferred to the adjacent fjord. A percentage of the fjord sedimentation in the last two decades thus includes material eroded from bedrock and stored in the landscape during the previous glacial expansions. Distal deltaic deposits extend across the fjord floor and likely interfinger with distal proglacial deltaic deposits sourced from the Tyndall Glacier. A paraglacial landscape response, such as the one exhibited in upper Taan Fjord where sediment delivery to fjords from tributary sources in synchrony with sediment produced by primary bedrock erosion by glaciers, helps to explain the order-of-magnitude discrepancy between sediment yields from Alaskan tidewater glaciers on 10^0- to 10^2-year timescales and sediment yields and exhumation rates on 10^4- to 10^6-year timescales.

Keywords: Paraglacial; Erosion rates; Sediment yield; Alaska; Landscape evolution; Deglaciation

1. Introduction

Deglaciation inevitably produces a geomorphic response in the landscape because glaciers act as base level for non-glaciated hillslopes and tributaries and because formerly glaciated portions of the landscape are subject to fluvial and hillslope processes after glacier retreat (Fig. 1) (Church and Ryder, 1972; Harbor and Warburton, 1993; Ballantyne, 2002). Fluvial incision into glacial valley bottoms, landsliding on over-steepened glacial valley walls, and remobilization of sediment stored non-glaciated tributary valleys create a sediment pulse from within glaciated basins that decays with time following glacial retreat (the so-called paraglacial period; Ballantyne, 2002). Erosion within formerly glaciated trunk and tributary valleys and sediment transfer out of basins is represented by a period of enhanced sediment accumulation in fjords and other sediment sinks. In landscapes where glaciers

* Corresponding author. Tel.: +1 541 737 1214; fax: +1 541 737 1200.
E-mail address: meigsa@geo.oregonstate.edu (A. Meigs).

0169-555X/$ - see front matter © 2006 Elsevier B.V. All rights reserved.
doi:10.1016/j.geomorph.2006.01.029

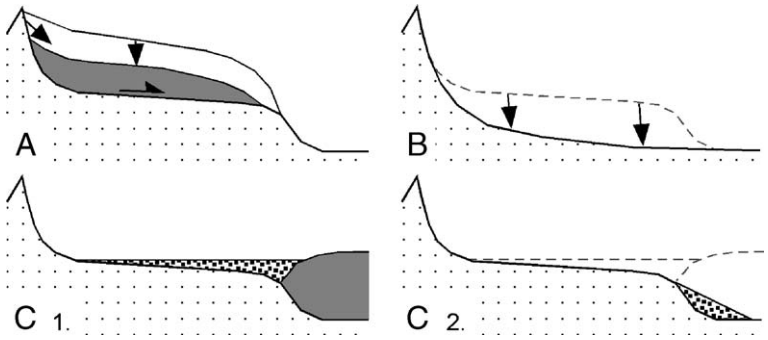

Fig. 1. Conceptual models depicting potential sources of sediment in glaciated basins. Sources include (A) erosion of cirque headwalls, valley walls, and the glacier bed (arrows); (B) fluvial modification of glaciated valleys; (C) transfer of stored material (1) to adjacent basins following glacial retreat (2).

retract but do not disappear during glacial minima, these nonglacial sediment sources add to the volume of sediment produced by glaciers over the same time span. Sediment sources within glaciated basins thus vary in space on glacial maxima–glacial minima timescales (Evenson and Clinch, 1987; Powell and Molnia, 1989; Cowan and Powell, 1991).

Taan Fjord, an arm of Icy Bay in the active Chugach/St. Elias orogenic belt in southern Alaska, has been created as the consequence of the dramatic retreat of the Tyndall Glacier over the past 50 years (Fig. 2) (Porter, 1989; Meigs and Sauber, 2000). The terminus has retreated ~10 km in the upper reach of Taan Fjord since 1983. Continuous sedimentation in the fjord has accompanied glacier retreat, sedimentation that is interpreted to be dominated by output from glacier termini (Molnia, 1979; Jaeger and Nittrouer, 1999; Koppes and Hallet, 2002). Analysis of aerial photographs from 1978, 1983, and 1996, field mapping, and topographic and bathymetric profiling are combined in this study to quantify the magnitude of sediment input into the fjord from sources other than the Tyndall Glacier. These data reveal a dramatic and rapid landscape response to the Tyndall Glacier retreat, the consequence of which has been a commingling of sediment derived from four tributary valleys and the Tyndall Glacier following opening of the upper fjord between 1983 and 1996. The paraglacial landscape response, forced by retreat, affects fjord sedimentation, sediment sources, timescales and rates of sediment routing, and glacial landscape evolution. Moreover, consideration of sediment contributed from tributary valleys to fjords that include active trunk tidewater glaciers resolves, in part, discrepancies between sediment volume-based glacial erosion rates calculated on short 10^0- to 10^2-year timescales (Hallet et al., 1996; Koppes and Hallet, 2002) and sediment yields and exhumation rates on 10^4- to 10^6-year timescales (Jaeger and Nittrouer, 1999; Sheaf et al., 2003; Spotila et al., 2004).

2. Glacial retreat in Icy Bay

Icy Bay did not exist at the beginning of the twentieth century according to coastal explorers; the terminus of a glacier system comprising the individual glaciers in each arm of the bay occupied the modern bay mouth (Molnia, 1986; Porter, 1989). Taan Fjord, one of the four arms of Icy Bay, was created by the isolation of the Tyndall Glacier from the glacier system after 1960 (Fig. 2). Retreat of the Tyndall Glacier up Taan Fjord occurred in three stages. The terminus retreated ~6 km up-fjord (~0.6 km/year) between 1960 and 1969 (Porter, 1989). Aerial photos taken in 1983 show the terminus ~2 km up-fjord from its position in 1969, indicating a slowing of the retreat rate to ~0.15 km/year. A rate increase from 1983 to 1996 of ~0.8 km/year was followed by stabilization of the terminus ~10 km farther up the fjord by or before 1996. Bedrock outcrops in the center of the fjord in the 1969–1983 terminus region and an icefall with ~450 m of relief at the present terminus position suggest that bedrock highs and steps in the longitudinal profile of the valley floor modulated the retreat rate.

3. Methods

Landscape evolution in response to retreat of the Tyndall Glacier was quantified by a number of methods. Bedrock units, structural data, geomorphic surfaces, modern and abandoned channels, and landslides were mapped at 1:24,000 on aerial photographs taken in 1996 (Fig. 3). Field observations and sedimentologic description provided characterization of the geomorphology in

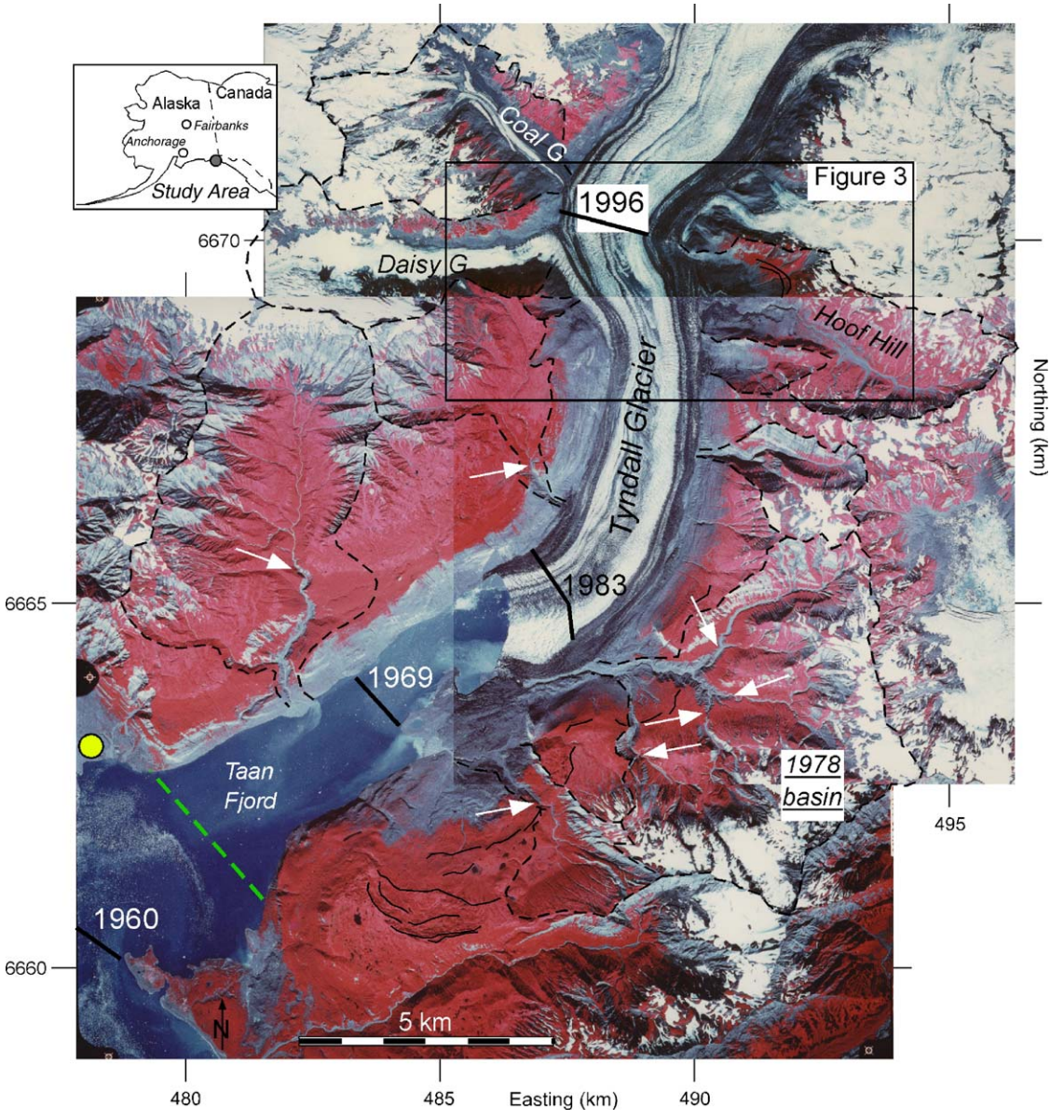

Fig. 2. False color air photo of Taan Fjord in 1978. Fjord outlet indicated by dashed green line. Thick black lines across fjord mark terminus position of Tyndall Glacier in 1960, 1969, 1983, and 1996 (see Porter, 1989 and Fig. 3). Drainage divides for tributary basins outlined with dashed lines. Tyndall Glacier lateral moraines marked by arcuate black lines near bedrock (grey)–vegetation (red) break on the eastern wall of fjord. Yellow dot west of fjord outlet indicates ice-free area between late Holocene glacial advances (Porter, 1989). White arrows identify knickpoints in tributary rivers. Inset map shows location of study area in southern Alaska. Fig. 3 location shown for reference.

the four tributary valleys (Figs. 4–7). Landscape changes between 1978 and 1996 were constrained by comparison of 1978, 1983, and 1996 air photos (Fig. 5). A GPS/fish-finding sonar was used to make depth measurements in Taan Fjord. Position and individual points have an average spacing of ~5.4 m (Figs. 8 and 9). Depth errors are <±5 m, based on the tidal range in the fjord (~3 m), and replicate measurements of selected points. Limited portions of the fjord are poorly imaged because of the concentration of ice discharged by calving by a persistent SE-directed brackish-water input. Alluvial fan surfaces and modern stream profiles were measured with a laser range-finding device and a hand-held GPS unit (Fig. 9). Angular and distance errors of the laser range finder are ±0.4° and ±0.15 m, respectively.

4. Geomorphology and post-1978 landscape change

The valley system in upper Taan fjord is inset into bedrock comprised of deformed Cenozoic sedimentary strata. North-dipping fluviodeltaic deposits of the Eocene Kultieth Formation (Plafker, 1987) are in thrust contact with north-dipping Pliocene–Pleistocene glaciomarine Yakataga Formation bedrock (Lagoe et al., 1993; Zellers, 1993) in the Tyndall Glacier terminus region (Fig. 3). Surficial fluvial, glacial, and hillslope deposits unconformably overlie these bedrock units and were deposited by glaciers, rivers, hillslope processes, and landsliding.

4.1. West side tributaries

All tributaries at the head of Taan Fjord have evolved as Tyndall Glacier thinned and retreated (Figs. 2 and 3). Two glacial and one fluvial tributary deliver sediment to the fjord from the west (Fig. 3). Glaciers in the Daisy and Coal basins were tributaries to the Tyndall Glacier as recently as 1983 (Fig. 2) and retreated into their respective valleys by 1996 (Figs. 3 and 4). Both glaciers now occupy hanging valleys and the topographic inflections between each tributary valley and the fjord wall are elevated more than 450 m asl (Fig. 4A). A poorly sorted, blocky unconsolidated deposit comprised of angular clasts overlies Yakataga Formation bedrock downstream of the terminus of the Daisy Glacier (Figs. 3 and 4C). This veneer of sediment is interpreted as a recessional moraine, which is part of a geomorphic surface created during retreat and isolation from the Tyndall Glacier (surface T_3; Fig. 3). A similar deposit downstream from the Coal Glacier terminus mantles Kultieth Formation bedrock (Figs. 3 and 4D). Proglacial rivers emerging from beneath stagnant ice-cored moraines have incised through the thin veneer of recessional moraine into bedrock downstream of the termini of both glaciers (Fig. 4C,D). Farther downstream, across the hanging-trunk valley junction, the Daisy and Coal Rivers have steep channels and have cut narrow slot canyons into bedrock, in which relief in the gorges exceeds 60 m locally (Fig. 4A).

There are 2 principal nonglacial sediment sources on the western side of the fjord: a large-scale landslide of the interfluve between the Daisy and Coal basins (~800 m high, 500 m wide) and the steep fluvial catchment Camp Creek basin (Fig. 3). Extensive exposure of Yakataga Formation bedrock characterizes the Camp Creek basin (Fig. 3). Topographic relief in the basin is ~700 m between the headwaters and the fjord. There is no evidence of glacial occupation (moraines, till, kame terraces, etc.) in the drainage. A glacier was not present in the basin in 1978 (Fig. 2). Retreat of the Tyndall Glacier to its present position was accompanied by formation of a deep-seated bedrock landslide in the Yakataga Formation on the ridge separating the Daisy from the Coal Glacier (compare Figs. 2 and 3) (Meigs

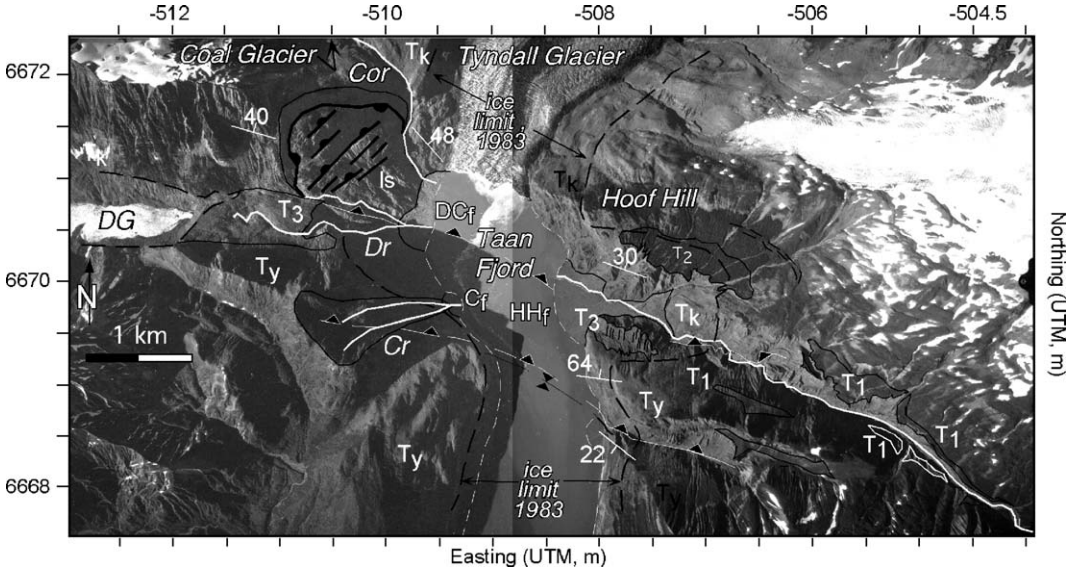

Fig. 3. (A) Map of upper Taan Fjord on 1996 air photo. Tyndall Glacier height in 1983 marked by black dashed line. Rivers (solid white lines): Camp (Cr), Daisy (Dr), and Coal (COr). Dashed white line is shoreline. Geomorphic surfaces: $T_{1, 2, 3}$. Camp fan (C_f), Daisy–Coal fan (DC_f), and Hoof Hill fan (HH_f). Moraines: short black lines. Bedrock units: Kultieth Formation (T_k) and Yakataga Formation (T_y). Thrust faults: thin white barbed dashed line. Landslide and scarps: solid black lines with half-ball. Shoreline marked by thick line.

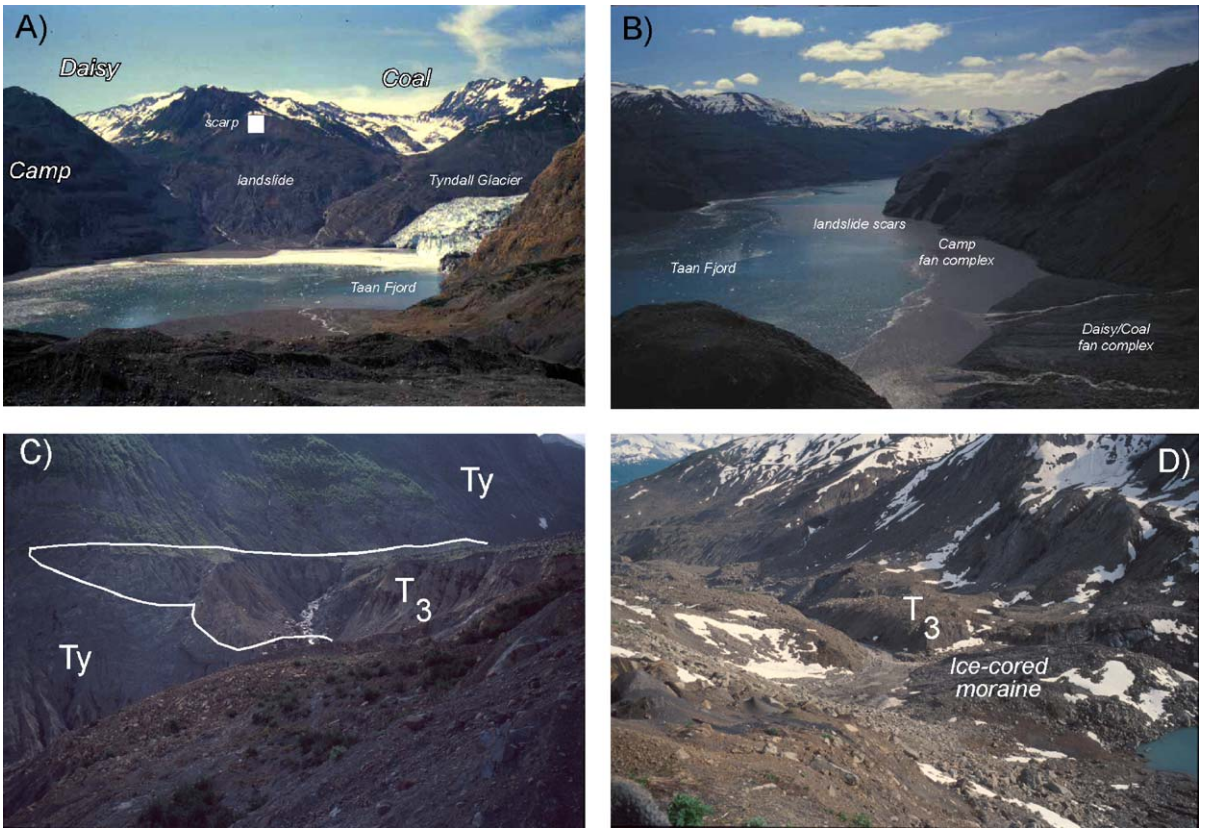

Fig. 4. Photographs of the Daisy and Coal drainage basins. (A) View looking west to the Daisy and Coal outlet streams. Note that both streams occupy steep, narrow gorges incised into bedrock. The eastern face of the interfluve between the two drainages is the site of a post-retreat landslide (see Fig. 2 and Meigs and Sauber, 2000). (B) View looking south across the Daisy/Coal fan delta complex. Brown water is interpreted to be hypopicnal flow of brackish water carrying suspended sediment from the Tyndall Glacier terminus, the Coal, and the Daisy streams. (C) View looking SW at the Daisy stream at the valley outlet. A thick white line marks the contact between a recessional moraine (T_3) formed after 1983 and the Yakataga Formation (T_y) bedrock. (D) View downstream to the SE of the Coal Glacier outlet stream incised into an ice-cored moraine near the glacier terminus and a recessional moraine formed after 1983.

and Sauber, 2000; Davis et al., 2002). Both the landslide itself and erosion of the landslide surface by debris flows and shallow channels transfer material into the fjord.

4.2. East side tributaries

The 12.4-km^2 Hoof Hill valley is the principal catchment on the east side of Taan Fjord (Fig. 3). A second, smaller basin lies to the south (Fig. 2). In 1978 the Tyndall Glacier flowed ~1 km eastward into the lower Hoof Hill valley (Fig. 5A). Comparison of 1978, 1983, and 1996 aerial photography and field observations indicates that the glacier surface elevation between 1978 and 1983 was roughly 390 m asl. By 1996 the Tyndall Glacier terminus had retreated to a position north of the outlet of the Hoof Hill River (Figs. 3 and 5). The lower Hoof Hill River presently occupies a canyon where the same reach flowed on a low-gradient alluvial bed at ~500 m asl as recently as 1983 (compare points 1 and 2; Fig. 5).

Whereas the lower Hoof Hill valley is deeply dissected, the upper part of the basin is U-shaped and the longitudinal profile is characterized by a steep headwall reach that becomes nearly flat downstream (Fig. 6E,F). In the upstream reach, the Hoof Hill River flows on top of an alluvial surface (Fig. 5B), which extended nearly to the margin of the Tyndall Glacier in 1978 (Fig. 5A). A >450-m-thick sequence of unconsolidated sand and gravel is exposed throughout the lower, dissected reach of the Hoof Hill river. These unconsolidated sediments unconformably overlie bedrock. Valley-parallel striations are preserved on the bedrock surface below the contact where exposed.

Three geomorphic surfaces, abandoned erosional or depositional surfaces, are preserved in the Hoof Hill

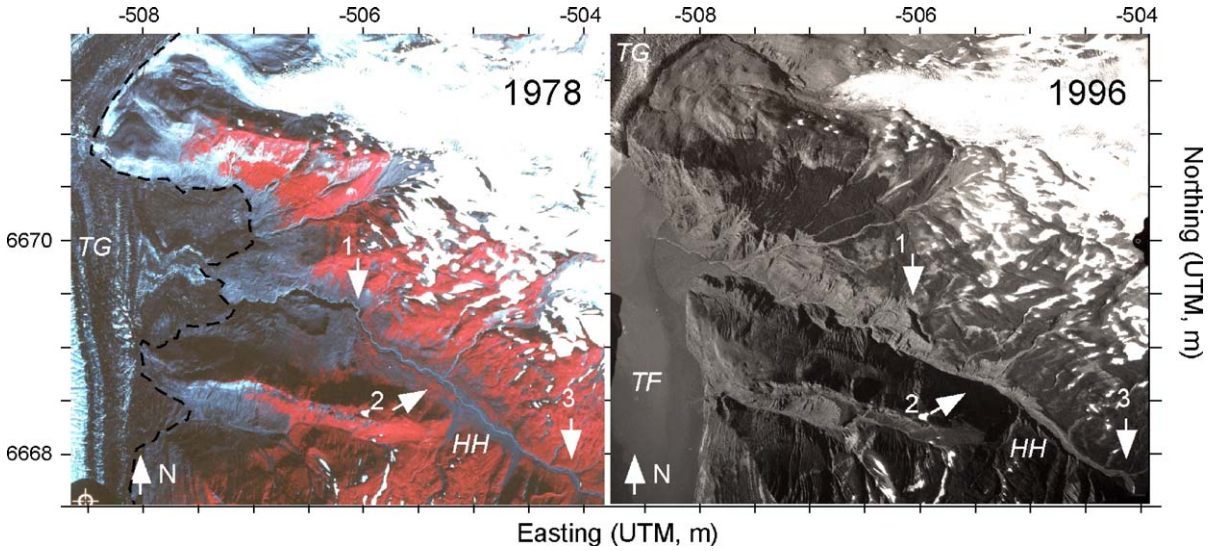

Fig. 5. Aerial photographs comparing Hoof Hill valley (HH) in 1978 (left) and 1996 (right). Numbers 1, 2, and 3 are reference points for comparison of the magnitude of change and knickpoint migration accompanying thinning and retreat of the Tyndall Glacier (TG) and the opening of Taan Fjord (TF). The knickpoint in the Hoof Hill River migrated 2.7 km from point 1 to point 3 between 1978 and 1996. Dashed line in the 1978 photo delineates the eastern margin of the Tyndall Glacier.

drainage (Fig. 3). T_1, the oldest and highest surface, sits above 500 m asl (Fig. 6A). T_1 is underlain by more than 450 m of unconsolidated alluvium and colluvium (Fig. 6B–F. Concave-to-the-west low-relief ridges occur at the same elevation (~500 m asl), but to the west of the T_1 surface. T_2 is a low relief surface present along the northern flank of the Hoof Hill River valley. The surface is inset and topographically lower than T_1. A <1–10-m-thick stratified boulder–cobble deposit underlies T_2. T_3, the youngest surface, is a discontinuous sloping, west-facing surface that extends from 410 to 45 m elevation and cross cuts the gravel lying below T_1. A series of parallel, north–south trending, 2- to 4-m-high gravel-cored ridges are present on T_3 between 410 and 90 m elevation (Fig. 3). These ridges parallel the trend of the east wall of Taan Fjord. Differential relief between the T_1 surface and the current channel increases from 0 m 2 km west of the headwaters to >100 m 5 km west of the headwaters (compare Fig. 6C–F).

The unconsolidated sediments underlying T_1 consist of a sequence of interbedded gravel and sand (Fig. 7). Most of the sediments are perched on the walls of the current river canyon and not accessible for close inspection. A measured section was constructed using the laser range finder to measure thickness at a series of four observation points. Thickness and the general characteristics of the strata were measured from each observation site. These strata are continuously exposed from ~45 m asl to the T_1 surface at ~500 m elevation (Fig. 6). Onlap onto an erosional surface on bedrock characterizes the basal contact of the sequence (Fig. 6B, C). Internally the sequence is stratified (Fig. 6C,D) and organized into 8- to 15-m-thick packages that fine upward from clast-supported cobble–boulder deposits to pebbly sands (Fig. 7). Basal contacts of each package undulate, with 1–5 m of relief, and are apparently erosional. Bedding is well developed in most of the packages (Fig. 6C,D). Two-to eight-meter-high cross strata are present throughout the section (Fig. 6B). Massive, poorly sorted ~10- to 30-m-thick angular cobble–boulder beds occur at the base, between 120 and 130 m and between 160 and 190 m (Fig. 7).

T_1 and the underlying strata are interpreted as a sequence of braided stream deposits that infilled a previously glaciated valley. Although moraines are present at the outlet of the Hoof Hill River on the west, these moraines are concave-west indicating that a west-flowing glacier in the Hoof Hill valley did not form them. These moraines are interpreted as lateral moraines formed on the eastern margin of the Tyndall Glacier (Fig. 3). Because the moraines and associated trimlines down fjord to the south are most likely related with the maximum extent of the Tyndall Glacier at the end of the nineteenth century, the moraine at 500 m is interpreted to have formed during the Little Ice Age advance. The gravel ridges on T_3 are interpreted to be recessional moraines formed from thinning and retreat of the eastern margin of the Tyndall Glacier. Together, these observations and interpretations suggest that the Tyndall Glacier margin acted as a dam to the flux of

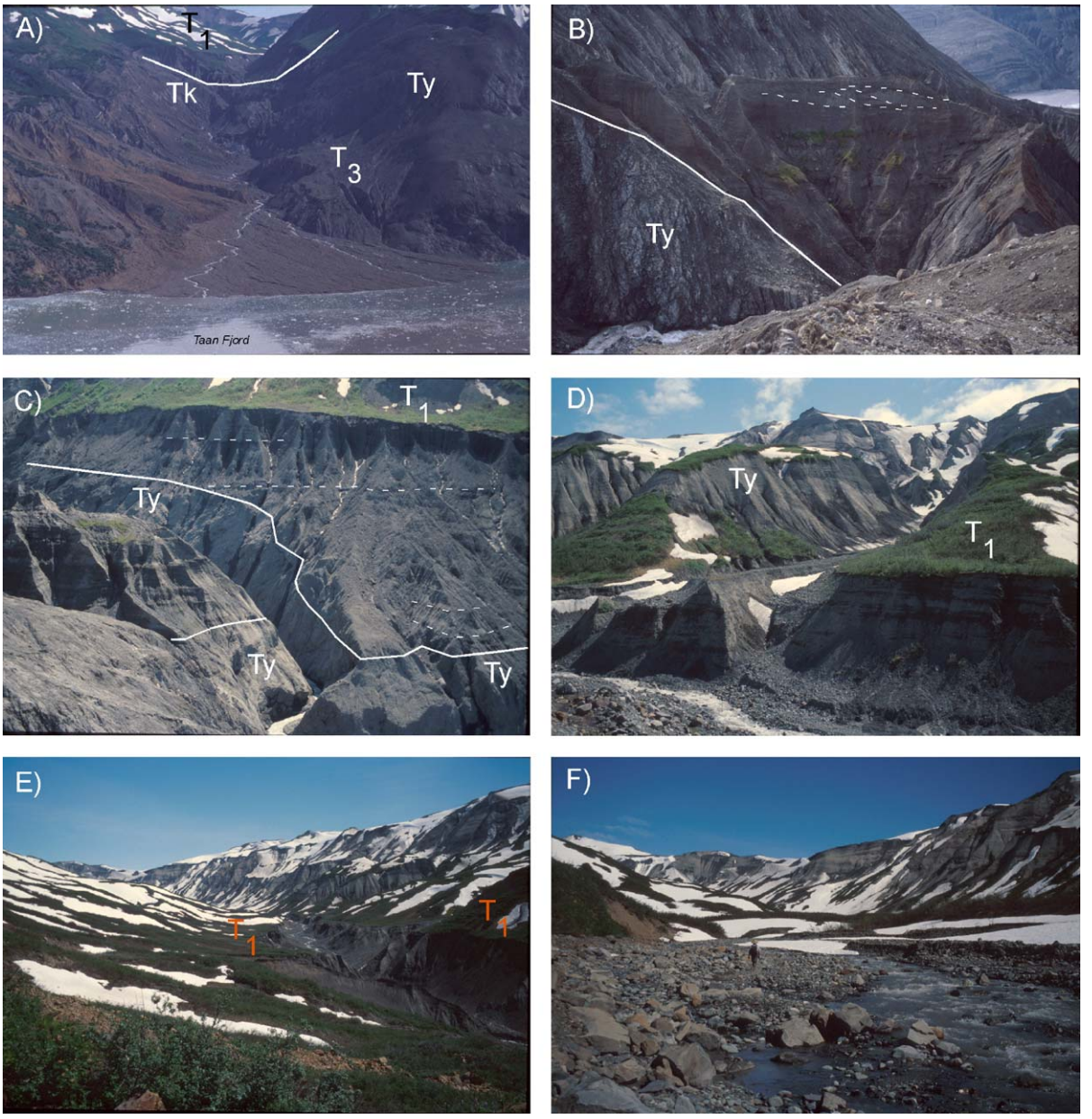

Fig. 6. Upstream changes in the Hoof Hill drainage basin. (A) View looking east across Taan Fjord at the Hoof Hill fan, T_1 and T_3, and Kultieth (T_k) and Yakataga Formations (T_y) bedrock. (B) Depositional contact between T1 gravel and T_y at km 4.2 (Fig. 10). Note the ~5-m-high cross-stratification, which represents either a delta front in an ice-marginal lake or lateral accretion surfaces of a side bar. Thickness of T_1 fill is ~450 m. (C) Onlap and upstream thinning of T_1 gravel at km 5.0 (Fig. 10) indicate back-filling of pre-existing paleorelief. Note the stratification. Decrease in differential relief between T_1 and the present Hoof Hill stream between river km 5.0 (C) and 6.0 (D). (E) View looking upstream from river km 6.0 to 7.5 illustrating the location of a knickpoint in 1998. (F) Upstream of km 7.5, the Hoof Hill stream flows on gravel bed surface of T_1.

sediment derived from within the Hoof Hill valley. Accordance of the elevation of the T_1 surface and a Tyndall Glacier lateral moraine indicates that aggradation of fluvially and hillslope-derived material was forced by a base level rise caused by glacial thickening as the Tyndall Glacier advanced downvalley and penetrated a short distance into the Hoof Hill valley in late Holocene glaciations.

There is no evidence that a tributary glacier occupied the Hoof Hill valley during the Little Ice Age. No moraines have been preserved on the surface of T_1 to the east of the Tyndall Glacier lateral moraine (Figs. 2 and

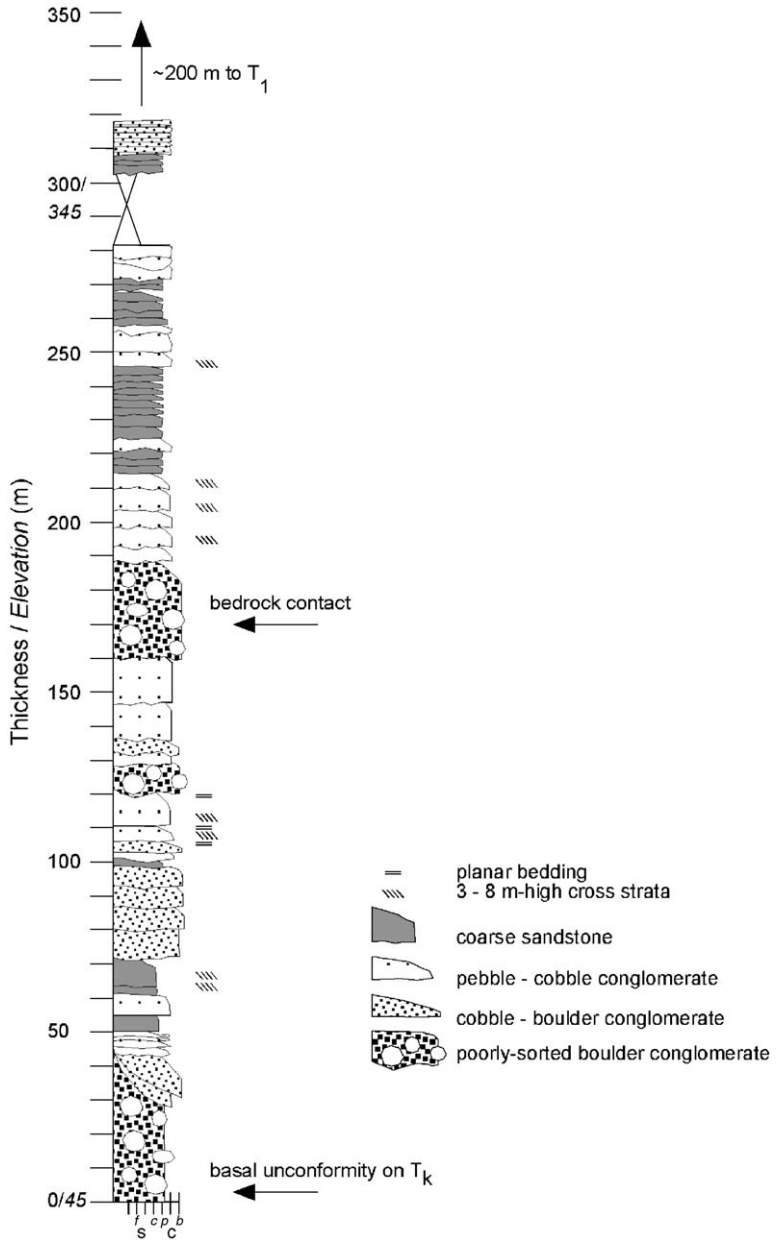

Fig. 7. Measured stratigraphic section through the unconsolidated sediments underlying T_1 in Hoof Hill valley. The base of the section occurs at ~43 m asl and unconformably overlies bedrock.

5). Relative to the elevation of valleys that supported glaciers during the Little Ice Age, the Hoof Hill valley is lower. The elevation of the headwaters of the Hoof Hill valley is ~600 m, whereas the headwaters of the Coal and Daisy valleys are above ~800 and ~900 m, respectively. Estimates of the modern equilibrium line altitude (ELA), snowline, and glaciation threshold all lie between 800 and 900 m for the Chugach/St. Elias Range at the latitude of upper Icy Bay (Péwé, 1975; Østrem et al., 1981; Mayo, 1986). ELAs during the Holocene are estimated to have been 150 to 200 m lower than at present (Calkin et al., 2001). The Hoof Hill valley, therefore, may not have been sufficiently high to support glacier formation. Whether glaciers occupied the valley during earlier Holocene advances is not clear. Whereas the massive, poorly sorted beds (Fig. 7) may represent till from either the Tyndall Glacier or from a tributary glacier within the Hoof Hill valley, the lack of evidence for glacial occupation in the valley implies that they likely represent debris flow deposits from the valley

walls. Regardless, material evacuated from the valley since 1996 (or earlier) is dominated by fluvial and colluvial sediments stored in the Hoof Hill valley over one or more late Holocene glacial advances.

4.3. Post-retreat sediment transfer to Taan Fjord

Fan deltas constructed between 1983 and 1996 are now present at all tributary valley outlets at the head of the fjord (Fig. 8). Sediment sources of the east side fan deltas are fundamentally different from those on the west because of differences in the geomorphology on the two sides of the fjord. On the west side, sediment comprising the Camp and Daisy–Coal fan deltas was derived primarily from bedrock eroded following opening of the last kilometer of Taan Fjord. Sediment from the Coal and Daisy catchments includes material produced by primary glacial and fluvial erosion of

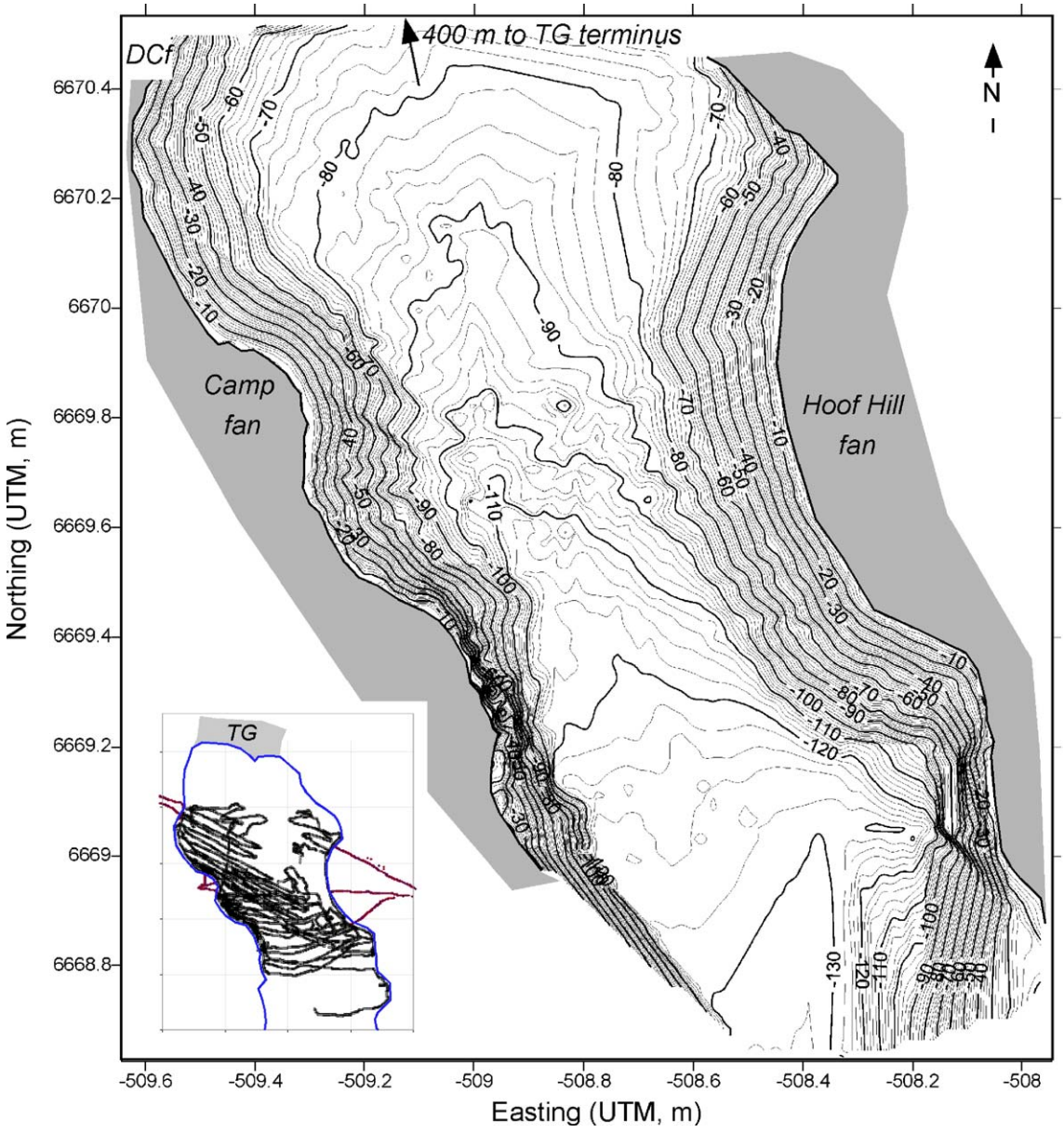

Fig. 8. Bathymetry of upper Taan Fjord. Submarine fans are associated with the Hoof Hill, Camp, and Daisy–Coal (DC_f) drainages. A large fan sourced from the terminus of the Tyndall Glacier (TG) occupies the northern end of the fjord. The heavy black line marks the shoreline and the grey shaded region is land. Contour interval is 10 m. Inset shows distribution of depth measurements, the coastline, and topographic profiles on the fans. White areas between the shoreline and data points in the north end of the fjord were inaccessible because of calved Tyndall Glacier ice.

bedrock and removal of the thin veneer of till (T_3) mantling bedrock (Fig. 4). Although the presence of deeply incised gorges downstream of both the Daisy and Coal Glaciers implies that fluvial incision of bedrock is an important source (Fig. 4A,C), the proportion of detritus in the fan delta complex derived from hillslope and fluvial sources relative to glacial sources is unknown. Fluvial and mass-wasting erosion of the landslide in the interfluve between the Coal and Daisy basins also contributes material to the fan delta complex. Hillslope and fluvial processes produce sediment delivered from the Camp basin (Fig. 3). On the east side, two principal sources comprise the Hoof Hill fan delta. One major source is the wedge of fluvial and colluvial deposits that underlie T_1 (Fig. 6B–E). The second source is primary bedrock erosion of bedrock below the T_1–bedrock contact (Fig. 6B,C). Thus, the Hoof Hill fan delta consists of material derived from the fluvial erosion bedrock in the last 20–30 years and, importantly, stored material produced by bedrock erosion during the Little Ice Age and earlier Holocene advances.

The west-side fan delta complex has a smaller area (0.2 km^2) than the Hoof Hill complex on the east (0.4 km^2) (Figs. 3 and 8). A prominent break in slope occurs at the shoreline on each of the fan delta complexes (Fig. 9A–C). From the fan head on land to the delta toe, the surface slope is 6° to 11° between the head and the coast and decreases from 28°–18° to 0° systematically from the coast to the toe at the fjord center. Depth along the fjord centerline increases from −70 m roughly 0.4 km south of the Tyndall Glacier terminus to −130 m 1.1 km to the SSE (Fig. 9D). Both the cross-sections and map indicate that the Hoof Hill delta has apparently prograded across the fjord center line, which may have resulted in the commingling of the Camp and Hoof Hill delta bottom sets (Figs. 8, 9B). Iceberg discharge from the Tyndall Glacier limited the proximity to which the fjord near the terminus could be mapped. Clearly, a delta complex sourced from the glacier is prograding to the SE (Fig. 9D). Thus, material accumulating in the upper 3 km of the fjord since retreat of the glacier to its present position includes sediment derived from glacial erosion in the Tyndall Glacier basin, from fluvial erosion of bedrock in the Camp basin, from primary bedrock erosion by fluvial and glacial processes in the Daisy and Coal basins, and from erosion of stored older fluvial deposits and fluvial erosion of bedrock in the Hoof Hill basin. Deltaic bottom sets from each of these basins overlap in the upper fjord (Fig. 8). Fjord-bottom sediment volume in profile, therefore, cannot be simply inverted for the proglacial sediment flux and *basin-*

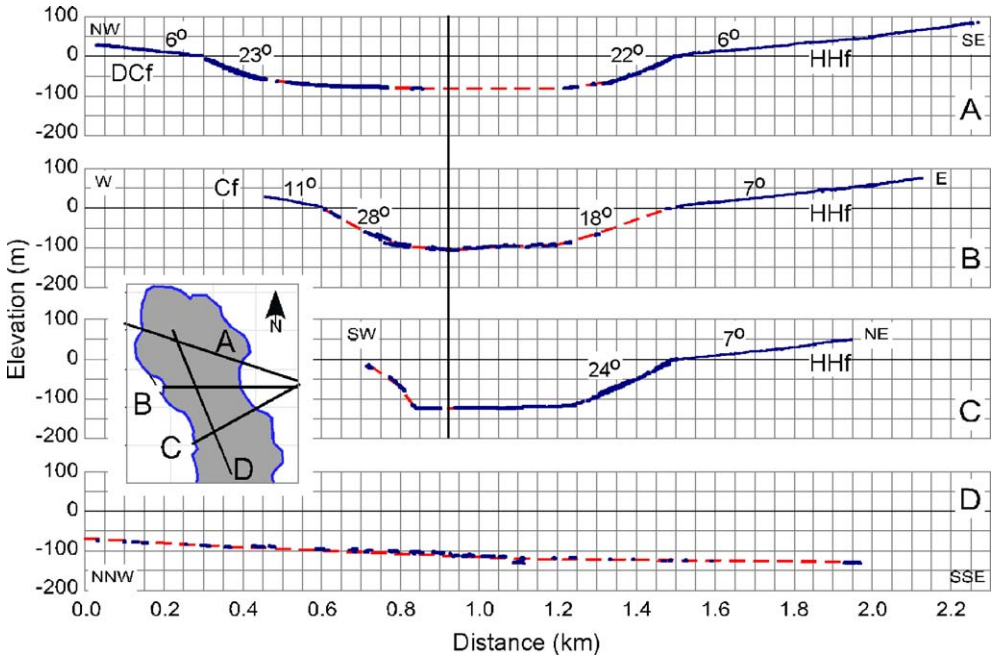

Fig. 9. Combined bathymetric and topographic profiles across Taan Fjord and fan delta complexes. (A) Hoof Hill–Daisy–Coal. (B) Hoof Hill–Camp. (C) Southeastern Hoof Hill. (D) Fjord centerline profile. Surface slopes are reported in degrees. Fjord morphology on the SW side of profile (C) is interpreted to represent sediment-free bedrock surface (solid). Sediment area (km^2) is material between the bedrock and the modern depositional surface with respect to fjord axis (line). Inset shows profile locations.

Table 1
Basin properties

Basin	Basin area (km^2)	Fan area (km^2)	Stored volume (km^3)	Eroded volume (km^3)
Coal	16.2	0.2[a]	0	0.01[b]
Daisy	15.4	0.2[a]	0	0.01
Camp	3.7	0.08	0	–
Hoof Hill	12.4	0.4	0.6	0.08

[a] Fan area includes both Coal and Daisy fans.
[b] Estimate.

average glacial erosion rate (i.e., Koppes and Hallet, 2002).

Differences in the size of fan delta complexes on the western and eastern sides of the fjord are consistent with the extent and volume of dissection of the source valleys (Table 1 and Fig. 3). Estimates of the missing volume from the valleys with preserved geomorphic surfaces highlight these differences and provide order-of-magnitude estimates of sediment storage volume and eroded volumes, fluxes, and basin-averaged erosion rates. A longitudinal profile from the drainage divide at the head of Daisy Glacier to the divide at the head of the Hoof Hill valley contrasts the western and eastern basins, respectively (Fig. 10). The missing material is represented in cross-section as the difference between the lower modern channel-valley profile and the upper profile, which is an abandoned geomorphic surface (T_3 on the west and T_1 and T_3 on the east). An order of magnitude more material has been removed in cross-section from the Hoof Hill valley (~0.4 km^2) than from the Daisy valley (0.05 km^2; Fig. 4). Geomorphic constraints combined with assumed simplified valley cross-sectional areas permit estimation of eroded volumes from the terrestrial basins.

The Hoof Hill River has cut a gorge through the T_1 surface, evacuated some of the T_1 fill, and is presently cutting into bedrock (Figs. 6 and 10). A knickpoint between T_1 and the modern channel occurs ~2.7 km upstream of the top of the T_3 surface (Fig. 10). A volume of stored fluvial deposits within the Hoof Hill valley can be estimated by assuming a half-conical shape to the stored material with a radius equal to half the width of T_1 at the outlet (Fig. 3) and a minimum length equal to the distance upstream to the knickpoint (Fig. 10). On the assumption that the stored volume has a half-cone shape, ~0.59 km^3 of sediment was stored in the Hoof Hill valley against the margin of the Tyndall Glacier. The missing volume of material, including both stored sediment and eroded bedrock, is at least 0.08 km^3, given that the width of the eroded area in 1996 was ~200 m (Figs. 3, 5) and that the current channel relief is ~100 m (Fig. 10).

In map view, T_3 is largely preserved in the Daisy Valley, the river is a slot canyon incised through bedrock, and a knickpoint between T_3 and the modern channel is ~500 m upstream of the top of T_3 (Figs. 3, 4). Knickpoint propagation upstream in the Daisy valley is

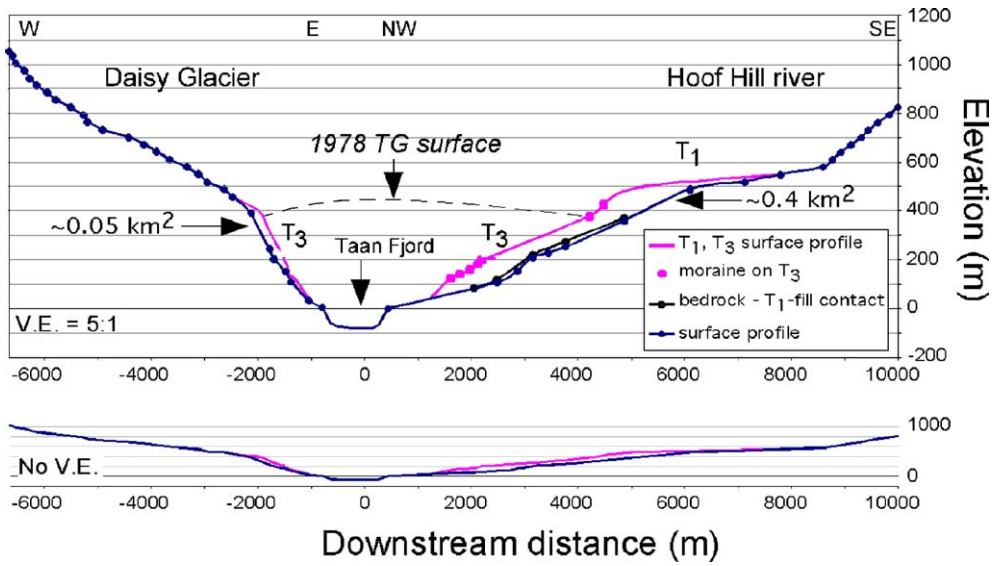

Fig. 10. Longitudinal profile from the head of Daisy Glacier to the head of the Hoof Hill valley. Present surface profile is indicated by lower line. Upper line represents abandoned T_1 and T_3 geomorphic surfaces. Middle line indicates bedrock contact at the base of T_1 fill in the Hoof Hill valley. Eroded area in cross-section is the difference between pink and blue lines. Dashed line in air represents schematically the Tyndall Glacier surface profile in 1983. Daisy and T_1 have glaciated valley profiles. Lower cross-section has no vertical exaggeration.

limited by the glacier terminus at km ~3.5 (Fig. 10), which effectively dictates how far upvalley a fluvial signal is transmitted. An eroded volume of 0.01 km^3 is suggested given the average 200-m canyon width in map view (Fig. 3) and the 0.05-km^2 area missing between the modern channel and T_3 (Fig. 10). A comparable amount has probably been removed from the Coal Glacier valley, although it is not possible to directly estimate because the 1996 air photo only covers a part of the valley (Fig. 3).

Whilst valleys in upper Taan Fjord have experienced a base level drop of at least 400 m since 1978 (Fig. 10), more material has been transferred from the Hoof Hill valley to Taan Fjord than the Daisy and Coal basins combined because of the greater erodibility of the unconsolidated T_1 fill in the Hoof Hill valley compared with the bedrock in the other valleys. Constraining the quantity of sediment evacuated by the rivers or the hillslopes from the Daisy and Coal Glaciers is not possible. The rate of downcutting by the Hoof Hill River may have decreased, however, after it encountered bedrock at the base of the fill.

5. Discussion

Sediment volumes from sinks within glaciated basins represent one of the primary data sets used to estimate primary bedrock erosion rates by glaciers (Molnia, 1979; Stravers and Syvitski, 1991; Hallet et al., 1996; Jaeger and Nittrouer, 1999; Koppes and Hallet, 2002). Sediment accumulated over the past 10^1 to 10^3 years in southern Alaskan fjords have very large volumes (ranging from $2–100\times10^6$ m^3 $year^{-1}$) (Molnia, 1979; Carlson, 1989; Powell and Molnia, 1989; Hallet et al., 1996; Hunter et al., 1996), which equate to basin-averaged erosion rates ranging from 5 to 60 mm $year^{-1}$ (Hallet et al., 1996). These rates exceed sediment yield rates on 10^4- to 10^5-year timescales determined from sediment thicknesses as deduced from seismic lines and cores (Jaeger and Nittrouer, 1999; Sheaf et al., 2003), exhumation rates measured on 10^6-year timescales derived from low-temperature thermochronometers (Johnston et al., 2004; Spotila and Meigs, 2004; Spotila et al., 2004), and estimates of tectonic influx and rock uplift rates in the Yakutat terrane foreland fold-and-thrust belt and backstop (Meigs and Sauber, 2000; Johnston et al., 2004; Meigs et al., 2004; Spotila et al., 2004).

One way to reconcile the observation that the *basin-average* sediment yield deduced from sediment thickness is greater over the last 10^2 years than over the last 10^4 years is to argue for an increase in erosion rates on 10^1- to 10^3-year timescales as the consequence of a climatically induced change in glacier sliding rate resulting from a short-term shift in glacier mass balance (Koppes and Hallet, 2002). Alternatively, stored sediment and a disequilibrium landscape response represent a potentially significant contributor of sediment to sinks (Church and Ryder, 1972; Church and Slaymaker, 1989; Harbor and Warburton, 1993; Ballantyne, 2002). The basin-averaged erosion rate for the Hoof Hill valley between 1983 and 1996, for example, is 50 mm/year (given an eroded volume of 0.08 km^3 and a basin area of 12.4 km^2). Clearly the sediment volume and associated rate reflect the combined effects of a short-lived landscape response to a 400-m base level fall, pronounced geomorphic disequilibrium accompanying upstream knickpoint migration, and of a high source area erodibility. The volume transferred to the fjord from the Hoof Hill valley to the fjord is dominated by sediment stored over one or more Holocene glacial fluctuations and the amount represented by primary bedrock erosion by fluvial processes is relatively small (Fig. 10). Bedrock erosion that produced the stored volume occurred, in part, during one or more earlier Holocene glacial maxima. Sediment yield and volumes in fjords and other sinks used by Hallet et al. (1996) and others to estimate *basin-average* glacial erosion rates likely include material derived from sediment stored in the landscape in addition to primary bedrock erosion by glaciers (Church and Ryder, 1972; Church and Slaymaker, 1989; Harbor and Warburton, 1993; Ballantyne, 2002).

Geomorphic reorganization as the consequence of thinning and retreat of the Tyndall Glacier and concomitant base level fall is the principal factor driving sediment production from tributaries in upper Taan Fjord. The glacier system in Icy Bay has been in retreat since ~A.D. 1904 (Molnia, 1979; Porter, 1989). The terminus of Tyndall Glacier is more than 50-km up-fjord from the A.D. 1904 position. Given that thickness change for glaciers is greatest in the terminus region (Paterson, 1994), the rate of base level fall for any tributary valley depends on its distance from the terminus. Base level fall rate in upper Taan Fjord must have changed from a low rate between 1904 and 1983 to a high rate between 1983 and 1996 as the terminus reached its present location. Those rates can be determined using the preserved geomorphic surfaces in the Hoof Hill valley and from changes in the Tyndall Glacier surface height in the 1976 and 1983 aerial photographs. T_1 is an aggradational surface graded to the maximum height of the Tyndall Glacier during the last advance. Thus, the glacier surface elevation lowered

from 490 m to ~390 m between 1904 and 1983 and from 390 m to sea level by 1996 (Fig. 4). Rate of base level fall, therefore, jumped from 1.3 m/year to 30 m/year before base level stabilized in 1996 or earlier. Modest incision of both the T_1 fill and T_3 surface on the 1983 and earlier photos supports this interpretation and suggests that tributary sources contributed a percentage of the material carried by the glacier prior to 1983. Since the Daisy and Coal Glaciers were still flowing into the Tyndall Glacier in 1983, the mode of sediment production from these tributary basins remained unchanged until rivers replaced glaciers in the lower reaches, which was followed by fluvial incision of bedrock (Fig. 4).

Do other tributary basins in the upper Taan Fjord reflect a similar response to Tyndall Glacier thinning and retreat? If a sediment pulse from tributary valleys is an important source of sediment to fjords during the paraglacial period, whether other basins preserve a geomorphic history similar to the basins in upper Taan Fjord represents a key question. Six basins (with areas that range from 3.8 to 19.6 km^2) in the lower Taan Fjord have knickpoints, evidence of steep, eroding valley bottoms, and fan deltas at their outlets (Fig. 2). The largest of these tributaries shows many similarities to the Hoof Hill basin. The "1978 basin" has an outlet that coincides with the 1978 Tyndall Glacier terminus position (Fig. 2). Key characteristics of the 1978 basin include flat, alluviated upper valley reaches, Tyndall Glacier lateral moraines at roughly the same elevation as the alluviated valley reaches; lower valley reaches characterized by steep, unvegetated valley bottoms; and prominent knickpoints separating the lower from the upper valley reaches. If the Hoof Hill valley represents an analog, the upper low gradient, alluviated valley bottom at the same elevation as an apparent lateral moraine suggests the presence of sediment stored against the margin of the Tyndall Glacier. A steep channel downstream of a knickpoint is indicative of the channel response to a base level fall accompanying thinning and retreat of the glacier past the outlet before 1978 (Fig. 2). Attempts to confirm these interpretations in the 1978 basin were thwarted by dense vegetation and impassable valley bottoms.

A general model summarizes the linkages between sediment production, routing, and landscape evolution of tributary valleys to glacier advance and retreat in Taan Fjord (Fig. 11). Aggradation–degradation cycles in tributary basins depend on a base level controlled by trunk glacier thickness variations in space and time. Assuming a constant sediment production rate in tributary valleys, the flux of material to adjacent fjords or trunk glaciers in time is a function of glacier advance–retreat rates and the tributary basin location relative to the trunk glacier terminus at glacial maxima and minima. Holocene deposits that suggest retraction of the terminus to a position at least ~25 km up-fjord from the mouth at 2000–1800 YBP and at 900–500 YBP (yellow dot, Fig. 2) (Porter, 1989) imply that the 1978 basin (located within ~30 km of the mouth of Icy Bay), for example, would experience repeated back filling and evacuation over Holocene glacial maxima/minima cycles, respectively (solid line, Fig. 11). Hoof Hill valley, which is ~50 km up-fjord, would have shorter cycles because of its greater distance from the glacial minima terminus position (Fig. 11). Total volume stored and evacuated would be sensitive to sediment production rates within the catchment, the duration of aggradation and degradation periods, and the sediment transport capacity of streams. Sediment

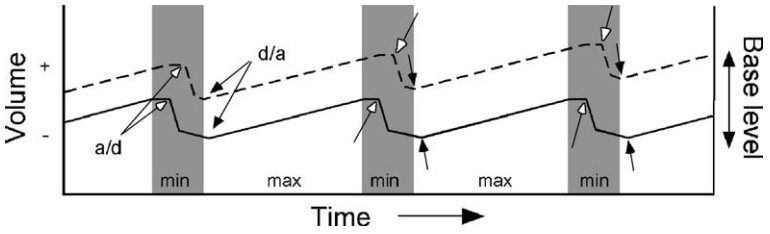

Fig. 11. Model of stored sediment volume and base level as a function of time for tributary basins at intermediate and large distances from a trunk glacier terminus at glacial maxima. The Tyndall Glacier terminus was ~30 km (solid line) and 50 km (dashed) from the 1978 and Hoof Hill basins, respectively, during Holocene glacial advances. Holocene glacial maxima in southern Alaska occurred between 3600–3400 YBP, 1500–1300 YBP, and 750–100 YBP (Little Ice Age) (Porter, 1989; Barclay et al., 2001; Calkin et al., 2001). Storage volume increase in tributaries is forced by base level rise accompanying glacier advance. Glacial retreat (grey shading) is accompanied by base level fall and erosion of sediment volume stored in tributaries, the magnitude of which is a function of the amount of stored material, the duration of the glacial minimum, and stream power. Note that aggradation/degradation (a/d; white arrows) and degradation/aggradation (d/a; black arrows) transitions are out of phase for the two basins because glacier thickening/thinning modulates base level, which varies in space and time as a function of glacier advance/retreat rates, respectively, and glacier surface profile.

delivery from such a basin to a trunk glacier or fjord has two time and volume scales. Partial evacuation of the tributary basin would result from glacier thinning at the valley mouth during short-period retreat. Near-complete evacuation is expected to occur only when the trunk glacier terminus retracts upvalley past the tributary valley junction.

6. Conclusions

Tributary valleys in the upper 10 km of Taan Fjord, an arm of Icy Bay on the south flank of the Chugach/St. Elias Range in southern Alaska, are responding to the retreat and stabilization of the Tyndall Glacier terminus to its present position in the last two decades. Landscape change was documented by a combination of interpretation of air photos taken in 1978, 1983, and 1996 and field mapping and characterization of the geomorphology of tributaries in the upper fjord. Key findings include the following:

(i) Retreat of the Tyndall Glacier has caused a >400 m base level fall for all tributary valleys along Taan Fjord.
(ii) Daisy and Coal Glaciers were tributaries to the Tyndall Glacier as recently as 1983. Presently, the two glaciers are confined to their respective valleys. Proglacial streams from each of the glaciers have cut slot canyons through glaciomarine and fluvial–deltaic Tertiary bedrock. Knickpoints in both the streams have reached the glacier termini.
(iii) Hoof Hill valley was occupied by a river in 1978 and probably throughout the Little Ice Age advance. More than 500 m of fluvial material aggraded in the valley against the eastern margin of the Tyndall Glacier during the Little Ice Age advance (and possibly previous advances). A knickpoint has migrated ~3 km upstream from the 1983 Tyndall Glacier margin and the channel has incised through the stored material into the underlying Tertiary bedrock.
(iv) Estimates of eroded volumes from the Daisy, Coal, and Hoof Hill Valleys are 0.01, 0.01, and 0.08 km^3, respectively. The eroded volume from the Daisy and Coal valleys represents primary bedrock erosion by rivers, whereas the eroded volume from the Hoof Hill valley is predominantly stored sediment produced by bedrock erosion during earlier glacial maxima. Roughly 0.5 km^3 of sediment remains stored in the Hoof Hill valley.
(v) Fan/deltas are building out from the outlets of each of these tributary valleys. The distal portion of the Hoof Hill fan interfingers with the distal portion of the Daisy, Coal, and Camp fans as well as the distal portion of a delta formed by the Tyndall Glacier.
(vi) Six additional tributary valleys show characteristics similar to the four basins of this study, including knickpoints separating deeply dissected lower reaches from undissected upper reaches, apparent sediment storage in valleys, and fan/deltas at their outlets.
(vii) A paraglacial landscape response resulting in a significant influx of sediment into fjords (including sources from stored sediment, primary bedrock erosion by rivers, and primary bedrock erosion by glaciers) may help to explain the large volumes of sediment in fjords and other sinks produced from within Alaskan glaciated basins.

Acknowledgements

Supported by NSF grant EAR-0001192 and NASA grant NASA (NAG-5-7646). Reviews of an earlier version of this manuscript by Mehgan Blair, Ross Powell, Suzanne Anderson, Bob Anderson, and an anonymous reviewer caused me to substantially rethink my interpretations. Dick Marston and 2 anonymous reviewers provided thoughtful reviews for this version of the manuscript. Danny Rosenkrans and Devi Sharp of the Warngell/St. Elias Park and Preserve were instrumental in facilitating this work.

References

Ballantyne, C.K., 2002. Paraglacial geomorphology. Quaternary Science Reviews 21, 1935–2017.
Barclay, D.J., Calkin, P.E., Wiles, G.C., 2001. Holocene history of Hubbard Glacier in Yakutat Bay and Russell Fiord, southern Alaska. Geological Society of America Bulletin 113 (3), 388–402.
Calkin, P.E., Wiles, G.C., Barclay, D.J., 2001. Holocene coastal glaciation of Alaska. Quaternary Science Reviews 20, 449–461.
Carlson, P.R., 1989. Seismic reflection characteristics of glacial and glacimarine sediment in the Gulf of Alaska and adjacent fjords. Marine Geology 85, 391–416.
Church, M., Ryder, J.M., 1972. Paraglacial sedimentation: a consideration of fluvial processes conditioned by glaciation. Geological Society of America Bulletin 83, 3059–3072.
Church, M., Slaymaker, O., 1989. Disequilibrium of Holocene sediment yield in glaciated British Columbia. Nature 337, 452–454.
Cowan, E.A., Powell, R.D., 1991. Ice-proximal sediment accumulation rates in a temperate glacial fjord, southeastern Alaska. In: Anderson, J.B., Ashley, G.M. (Eds.), Glacial Marine Sedimentation;

Paleoclimatic Significance. Geological Society of America, Boulder, CO, pp. 61–73.

Davis, K., Meigs, A., Krugh, W., 2002. Factor of safety implications from a slide caused by glacial erosion. Abstracts with Programs - Geological Society of America 34 (5), A-26.

Evenson, E.B., Clinch, J.M., 1987. Debris transport mechanisms at active alpine glacier margins: Alaskan case studies. Special Paper - Geological Survey of Finland 2, 111–136.

Hallet, B., Hunter, L., Bogen, J., 1996. Rates of erosion and sediment evacuation by glaciers: a review of field data and their implications. Global and Planetary Change 12, 213–235.

Harbor, J., Warburton, J., 1993. Relative rates of glacial and nonglacial erosion in alpine environments. Arctic and Alpine Research 25, 1–7.

Hunter, L.E., Powell, R.D., Lawson, D.E., 1996. Flux of debris by ice at three Alaskan tidewater glaciers. Journal of Glaciology 42 (140), 123–135.

Jaeger, J.M., Nittrouer, C.A., 1999. Sediment deposition in an Alaskan fjord: controls on the formation and preservation of sedimentary structures in Icy Bay. Journal of Sedimentary Research 69 (5), 1011–1026.

Johnston, S., Meigs, A., Spotila, J., Garver, J., 2004. Backstop and orogenic wedge cooling histories in the active Yakutat terrane collision, southern Alaska. Abstracts with Programs - Geological Society of America 36 (5), 270.

Koppes, M., Hallet, B., 2002. Influence of rapid glacial retreat on the rate of erosion by tidewater glaciers. Geology 30 (1), 47–50.

Lagoe, M.B., Eyles, C.H., Eyles, N., Hale, C., 1993. Timing of late Cenozoic tidewater glaciation in the far North Pacific. Geological Society of America Bulletin 105, 1542–1560.

Mayo, L.R., 1986. Annual runoff rate from glaciers in Alaska: a model using the altitude of glacier mass balance equilibrium. In: Kane, D. L. (Ed.), Cold Regions Hydrology Symposium. American Water Resources Association, Bethesda, MD, pp. 509–517.

Meigs, A., Sauber, J., 2000. Southern Alaska as an example of the long-term consequences of mountain building under the influence of glaciers. Quaternary Science Reviews 19, 1543–1562.

Meigs, A., Spotila, J., Johnston, S., Blair, M., 2004. Role of tectonics and climate in the topography, glaciation, denudation, and flow of rocks in the Chugach/St. Elias range (southern Alaska) active collisional orogen. Abstracts with Programs - Geological Society of America 36 (5), 307.

Molnia, B.F., 1979. Sedimentation in coastal embayments, northeastern Gulf of Alaska. Proceedings 11th Offshore Technology Conference I, 665–676.

Molnia, B.F., 1986. Glacial history of the northeastern Gulf of Alaska—a synthesis. In: Hamilton, T.D., Reed, K.M., Thorson, R.M. (Eds.), Glaciation in Alaska: The Geologic Record. Alaska Geologic Society, Anchorage, AK, pp. 219–235.

Østrem, G., Haakensen, N., Eriksson, T., 1981. The glaciation level in southern Alaska. Geografiska Annaler 63A, 251–260.

Paterson, W.S.B., 1994. The Physics of Glaciers. Elsevier, Tarrytown, NY. 480 pp.

Péwé, T.L., 1975. Quaternary Geology of Alaska. United States Geological Survey Professional Paper, vol. 835. Reston VA, 145 pp.

Plafker, G., 1987. Regional geology and petroleum potential of the northern Gulf of Alaska continental margin. In: Scholl, D.W., Grantz, A., Vedder, J.G. (Eds.), Geology and Petroleum Potential of the Continental Margin of Western North America and Adjacent Ocean Basins—Beaufort Sea to Baja California. Earth Science Series. Circum-Pacific Council for Energy and Mineral Resources, Houston, TX, pp. 229–268.

Porter, S.C., 1989. Late Holocene fluctuations of the fiord glacier system in Icy Bay, Alaska. Arctic and Alpine Research 21 (4), 364–379.

Powell, R.D., Molnia, B.F., 1989. Glacimarine sedimentary processes, facies and morphology of the south–southeast Alaska shelf and fjords. Marine Geology 85, 359–390.

Sheaf, M.A., Serpa, L., Pavlis, T.L., 2003. Exhumation rates in the St. Elias Mountains, Alaska. Tectonophysics 367 (1–2), 1–11.

Spotila, J., Meigs, A., 2004. Testing glacial limits to mountain building: the buzz saw in the Chugach/St. Elias Range, Alaska. EOS, Transactions—American Geophysical Union, Fall 2004 Abstracts with Programs 85 (47), T33D-03.

Spotila, J.A., Buscher, J.T., Meigs, A., Reiners, P.W., 2004. Long-term glacial erosion of active mountain belts: the Chugach/St. Elias Range, Alaska. Geology 32 (6), 501–505.

Stravers, J.A., Syvitski, J.P.M., 1991. Land–sea correlations and evolution of the Cambridge Fiord marine basin during the last deglaciation of northern Baffin Island. Quaternary Research 35 (1), 72–90.

Zellers, S.D., 1993. Controls on glacial–marine accumulation rates in the Yakataga Formation, Gulf of Alaska. GCSSEPM Foundation 14th Annual Research Conference Rates of Geological Processes, pp. 299–306.